

Preserved caudate function in young-onset patients with Parkinson's disease: a dual-tracer PET imaging study

Yu-jie Yang, Jing-jie Ge, Feng-tao Liu, Zhen-yang Liu, Jue Zhao, Jian-jun Wu, Yilong Ma, Chuan-tao Zuo and Jian Wang 

Ther Adv Neurol Disord

2019, Vol. 12: 1–11

DOI: 10.1177/
1756286419851400

© The Author(s), 2019.
Article reuse guidelines:
sagepub.com/journals-
permissions

Abstract: Parkinson's disease (PD) is a highly heterogeneous clinical entity. Patients with young-onset PD (YOPD) show some characteristic manifestations to late-onset PD (LOPD). The current study aimed to investigate the cerebral dopaminergic and metabolic characteristics in YOPD with positron emission tomography (PET) imaging. In our study, 103 subjects (42 YOPD and 61 LOPD patients) accepted both ^{11}C -N-2-carbomethoxy-3-(4-fluorophenyl)-tropane (^{11}C -CFT) and ^{18}F -fluorodeoxyglucose (^{18}F -FDG) cerebral PET imaging. Sixty-two patients out of 103 patients in our study completed the cognition tests. In this limited subsection, YOPD patients performed better in cognitive functioning than LOPD patients of similar disease duration. In ^{11}C -CFT imaging, dopamine transporter binding in caudate was relatively spared in YOPD compared with lesions in putamen. In ^{18}F -FDG PET, YOPD patients showed increased metabolism in basal ganglia relative to the healthy controls. When compared with LOPD patients, YOPD patients exhibited hypermetabolism in caudate and hypometabolism in putamen. Furthermore, the regional metabolic values in caudate correlated positively and moderately with the dopaminergic binding deficiency in caudate. The findings of this imaging study might offer new perspectives in understanding the characteristic manifestations in YOPD in light of better-preserved cognition function.

Keywords: age of onset, dopamine transporter, metabolic network, Parkinson's disease, positron emission tomography

Received: 31 October 2018; revised manuscript accepted: 25 April 2019

Introduction

Parkinson's disease (PD) is a highly heterogeneous neurodegenerative disorder with variable clinical features. This heterogeneity has prompted numerous classifications to delineate PD subtypes.¹ Although none of the proposed subtypes are robust enough to warrant formal delineation,¹ some suggest that young-onset and late-onset classification are acceptable in clinical practice.²

Patients of young-onset Parkinson's disease (YOPD) are more likely to have less severe initial motor symptoms, superior levodopa responsiveness,³ and relatively slower progression,³ but a great desire for life quality improvement.⁴ In advanced stages, YOPD patients are less likely to have gait disorders,⁵ but have a greater tendency

to develop motor complications.⁶ Moreover, YOPD patients suffer more from psychiatric symptoms, such as depression, anxiety, and visual hallucinations, but progress slower in cognitive dysfunction when compared with patients of late-onset Parkinson's disease (LOPD).^{7,8}

The above-mentioned clinical features of YOPD patients may suggest an etiologically different phenotype from LOPD. However, the underlying pathophysiological mechanisms remain unclear. As ^{18}F -fluorodeoxyglucose (^{18}F -FDG) is sensitive to regional metabolic changes, it can serve as a useful tool for the better understanding of molecular and synaptic activities in living human brains.⁹ In combination with ^{11}C -N-2-carbomethoxy-3-(4-fluorophenyl)-tropane

Correspondence to:

Jian Wang
and **Chuan-tao Zuo**

Department of Neurology
and National Clinical
Research Center for Aging
and Medicine, Huashan
Hospital, Fudan University,
12 Wulumuqi Zhong Road,
Jing'an District, Shanghai,
200040, China; Human
Phenome Institute, Fudan
University, 825 Zhangheng
Road, Pudong District,
Shanghai, 201203, China.
wangjian336@hotmail.com;
wangjian_hs@fudan.edu.cn;
zuochuantaofudan.edu.cn

Yu-jie Yang
Department of Neurology
and National Clinical
Research Center for Aging
and Medicine, Huashan
Hospital, Fudan University,
Shanghai, China

Feng-tao Liu
Department of Neurology
and National Clinical
Research Center for Aging
and Medicine, Huashan
Hospital, Fudan University,
Shanghai, China

Zhen-yang Liu
Department of Neurology
and National Clinical
Research Center for Aging
and Medicine, Huashan
Hospital, Fudan University,
Shanghai, China

Jue Zhao
Department of Neurology
and National Clinical
Research Center for Aging
and Medicine, Huashan
Hospital, Fudan University,
Shanghai, China

Jian-jun Wu
Department of Neurology
and National Clinical
Research Center for Aging
and Medicine, Huashan
Hospital, Fudan University,
Shanghai, China

Jing-jie Ge
PET Center, Huashan
Hospital, Fudan University,
Shanghai, China, and

Institute of Functional and Molecular Medical Imaging, Fudan University, Shanghai, China

Yilong Ma
Center for Neurosciences, Feinstein Institute for Medical Research, New York, USA

(^{11}C -CFT) positron emission tomography (PET) imaging, we aimed to explore the metabolic changes in cerebral regions and dopaminergic deficits in striatum in YOPD. This dual-tracer (^{18}F -FDG and ^{11}C -CFT) PET imaging study might be helpful to gain further insights into the underlying mechanisms in YOPD and its related clinical manifestations.

Methods

Participants

As we previously reported, between January 2010 and June 2014, 103 clinically diagnosed PD patients were consecutively recruited in this dual-tracer PET imaging study (DTPD Study) after signing an informed consent form in accordance with the Declaration of Helsinki.¹⁰ The diagnosis of PD was established by clinical examinations by two specialists of movement disorders according to the UK Brain Bank criteria.¹¹ In the current study, and in accordance with our previous study and previous reports,^{12,13} we define YOPD as patients with an age of onset of less than 50 years old.¹⁴ Therefore, this cohort was divided into 42 YOPD and 61 LOPD patients.

In addition, 103 healthy controls (42 participants younger than 50 years and 61 participants older than 50 years) were recruited for ^{18}F -FDG PET imaging; 43 of these independent healthy controls (13 participants younger than 50 years and 30 participants older than 50 years) were recruited for ^{11}C -CFT PET imaging. The study (approval number KY2016-214) was approved by the Human Studies Institutional Review Board, Huashan Hospital affiliated to Fudan University.

Clinical examinations

All patients were off anti-Parkinsonian medications for at least 12 h prior to clinical assessment and PET scans. Consecutive full neurological examination was performed to obtain a thorough assessment of patients' clinical data. "Off" state Hoehn and Yahr (H&Y) score and Unified Parkinson's Disease rating scale (UPDRS)¹⁵ motor score were evaluated. Medication history was documented and further converted to standard levodopa equivalent daily dosage (LEDD) for statistical analysis. After the clinical assessment, all subjects were scanned with ^{11}C -CFT PET, and scanned again with ^{18}F -FDG PET at the same time on the following day.

Cognition assessment

In a subsection of our study, 62 patients had cognition tests results. The global cognitive function was assessed using the Mini Mental State Examination (MMSE). The different cognitive domains, including attention, executive function, memory, visuospatial function, and language, were evaluated as suggested by Movement Disorders Society.¹⁶ In detail, the cognition tests performed in our study included Trail Making Test part A (TMT-A),¹⁷ Symbol Digital Modalities Test (SDMT),¹⁸ Stroop Color-Word Test part C (CWT-C),¹⁹ Trail Making Test part B (TMT-B),¹⁷ Rey Auditory Verbal Learning Test (AVLT),²⁰ delayed recall of the Rey-Osterrieth Complex Figure Test (CFT),²¹ Clock Drawing Test (CDT), Rey-Osterrieth Complex Figure Copy Test (CFT),²¹ Boston Naming Test (BNT), and Verbal Fluency Test (VFT).²²

PET imaging and processing

PET scanning was performed with a Siemens Biography 64 PET/CT (Siemens, Munich, Germany) in three-dimensional (3D) mode.^{14,23} Resting state brain scans were acquired with the subjects remaining in a quiet and dimly lit room. A CT transmission scan was performed first for photon attenuation correction.

The ^{11}C -CFT imaging process and data acquisition were performed as described previously.¹⁴ In short, ^{11}C -CFT images were acquired 60–80 min after intravenous injection of ^{11}C -CFT (350–400 MBq) and reconstructed with the ordered subset expectation maximization (OSEM) method. Prior to the ^{18}F -FDG PET imaging, all subjects were asked to remain a fasting state for at least 6 h. The emission scan, lasting for 10 min, was acquired 45 min after intravenous injection of ^{18}F -FDG (150–200 MBq) and reconstructed with the OSEM method. ^{18}F -FDG images were used as relative measures of regional glucose metabolism. Scans from each subject were spatially normalized and smoothed (Gaussian filter of 10 mm full width at half maximum) as described previously.²⁴

Data analysis

Both ^{11}C -CFT and ^{18}F -FDG PET data were analyzed using Statistical Parametric Mapping (SPM5) software (Wellcome Department of Imaging Neuroscience, Institute of Neurology,

London, UK) implemented in Matlab 7.4.0 (Mathworks, Sherborn, MA, USA).

In ^{11}C -CFT PET imaging analysis, a template for spatial normalization was created using ^{11}C -CFT PET and MR T1 images of 16 healthy controls as reported previously.²⁵ First, ^{11}C -CFT PET images were coregistered with the corresponding MR T1 images. Then, the spatial normalization parameters of each MR image in the Montreal Neurological Institute (MNI) space were applied to the coregistered ^{11}C -CFT PET image. Finally, the averaged PET image was smoothed using a 10 mm FWHM Gaussian kernel to serve as the template for normalization.

The ^{11}C -CFT PET images of the PD patients were spatially normalized with the template and then smoothed. To quantify striatal ^{11}C -CFT binding in individual patients, standardized regions of interest (ROIs) for the caudate, anterior putamen, posterior putamen, and occipital cortex were placed on the mean image summed over central slices,^{14,26} using ScAnVp software version 5.9.1 (Centre for Neuroscience, Feinstein Institute for Medical Research, Manhasset, NY, USA). For each ^{11}C -CFT PET scan, caudate and putamen dopamine transporter (DAT) binding was estimated for each hemisphere by the striatal-to-occipital ratio (SOR), defined as (striatum-occipital)/occipital radioactivity counts, and these values were averaged across hemispheres.²⁵

In ^{18}F -FDG PET imaging analysis, scans were spatially normalized into MNI brain space using a default PET template in SPM with linear and nonlinear 3D transformations. They were then smoothed by a Gaussian filter of 10 mm width over a 3D space to increase signal-to-noise ratio for statistical analysis. A voxel-based comparison using two-sample *t*-test according to the general linear model was performed. The contrasts for the decreased and increased metabolism were set as [1 -1] and [-1 1]. Mean signal differences over the whole brain were modeled by ANCOVA per subject. All the clusters that satisfied three criteria were presented: (1) significant with a voxel-wise threshold at $p < 0.001$ (uncorrected) over whole-brain regions; (2) had an extent threshold exceeding several times the average cluster size determined by the model; and (3) survived a Family-Wise-Error (FWE) correction at $p < 0.05$. The FWE-uncorrected clusters that survived only at $p < 0.001$ were accepted only in

hypothesis-testing analysis basing on previous studies. The SPM maps of altered glucose metabolism were finally overlaid on a standard T1-weighted magnetic resonance imaging (MRI) brain template for cluster localization.

To quantify the metabolic values in specific regions, we constructed a 4-mm radius spherical volume of interest (VOI) in the image space, centered at the peak voxel of clusters (Right Caudate [12, 8, 8] and Right Putamen [28, -20, 14]) that were significant in each SPM analysis. We then calculated the globally adjusted relative regional glucose metabolism (rCMRglc) to account for this variable in blood samples in YOPD patients and LOPD patients using ScanVP software (Version 5.9.1; Center for Neuroscience, the Feinstein Institute for Medical Research, Manhasset, NY, USA) as described previously.²⁴ The individual metabolic values of each region were then expressed as a percentage of whole-brain metabolism (metabolic value = [VOI value/whole-brain metabolism] $\times 50 \times 100\%$).

Statistical analysis

Differences in demographic and clinical features of the two groups (YOPD and LOPD) were analyzed using independent two-tailed *t*-test, Mann-Whitney *U* test, or chi-square test as appropriate. Dopaminergic binding of ROIs and metabolic values of VOIs between groups were compared with an independent two-tailed *t*-test. Correlation analysis between the metabolic values of VOIs and DAT binding values was performed using general linear model. All analyses were performed using SPSS 22.0 (SPSS Inc., Chicago, IL), and a two-tailed *p* value of less than 0.05 was considered significant.

Results

Demographic and clinical characteristics

A total of 103 patients were recruited in this study, with 42 in the YOPD group and 61 in the LOPD group. There was no significant difference between groups regarding gender, disease duration, H&Y stages, UPDRSIII scores and LEDD (Table 1). The demographic and clinical information of PD patients who performed cognitive tests and those without cognitive tests are shown in Supplementary Table S1. In brief, YOPD patients performed better in cognitive tests,

Table 1. Demographics and clinical characteristics of YOPD and LOPD patients.

	YOPD	LOPD	<i>p</i> value
Participants (Male/Female)	42 (26/16)	61 (39/22)	0.834 ^a
Age at examination	42.6 ± 8.7	62.0 ± 6.3	<i>p</i> < 0.001
Age of onset	39.6 ± 8.5	59.5 ± 6.5	<i>p</i> < 0.001
Disease duration (month)	27.0 (12, 52)	19.5 (12, 38.3)	0.337 ^b
Hoehn & Yahr stage	1.8 ± 0.8	1.8 ± 0.8	0.724
UPDRS III score (Off medication)	23.6 ± 12.9	21.0 ± 10.5	0.256
LEDD (mg/day)	300 (0, 500.3)	200 (0, 300)	0.291 ^b
MMSE (<i>n</i>)	28.0 ± 2.5 (28)	27.8 ± 2.84 (34)	0.725
CWT-C (<i>n</i>)	47.6 ± 3.0 (24)	45.5 ± 6.4 (31)	0.863*
TMT-A (<i>n</i>)	49.0 ± 18.9 (23)	67.2 ± 30.0 (33)	0.013*
SDMT (<i>n</i>)	44.7 ± 13.8 (23)	31.8 ± 12.7 (33)	0.001**
TMT-B (<i>n</i>)	131.0 ± 41.7 (23)	189.7 ± 80.6 (33)	0.001
AVLT (<i>n</i>)	6.3 ± 1.9 (24)	4.7 ± 2.9 (34)	0.015
DAT binding ^c			
Caudate	1.3 ± 0.4	1.2 ± 0.3	0.013
Anterior Putamen	0.9 ± 0.3	0.9 ± 0.3	0.599
Posterior Putamen	0.5 ± 0.2	0.6 ± 0.2	0.761
Data are given as mean ± standard deviation, and disease duration and LEDD are given as median (interquartile range). The data were compared between the two groups using independent-samples <i>t</i> -test. <i>p</i> values for the comparison of cognitive test scores between PD and control groups. * <i>p</i> < 0.01 in covariance analysis adjusting for age; ** <i>p</i> < 0.05 in covariance analysis adjusting for age. YOPD: Young-onset Parkinson's disease; LOPD: Late-onset Parkinson's disease; UPDRS: unified Parkinson's Disease rating scale; LEDD: levodopa equivalent daily dosage; MMSE, Mini Mental State Examination; CWT-C, Stroop Color-Word Test part C; TMT, Trail Making Test; SDMT, Symbol Digit Modality Test; AVLT, Auditory Verbal Learning Test; DAT, dopamine transporter; PDRP, PD related pattern.			
^a Chi-square test was performed.			
^b Mann-Whitney <i>U</i> test was performed. <i>p</i> values for the comparison between the YOPD and LOPD groups			
^c Left and right average value.			

including the TMT-A and SDMT in attention domain, TMT-B in execution domain, and AVLT in memory domain (Table 1 and Supplementary Table S3). After adjusting the age effects, the CWT-C in execution domain, and TMT-A and SDMT in memory domain were still better performed in YOPD than the LOPD (Table 1 and Supplementary Table S3). Demographic information on the healthy control participants in ¹⁸F-FDG or ¹¹C-CFT PET imaging can be found in Supplementary Table S2.

Dopaminergic imaging difference between YOPD and LOPD

In the ¹¹C-CFT PET imaging study, the DAT binding (ROIs) in caudate, anterior putamen and posterior putamen in both YOPD and LOPD groups decreased significantly compared with the age-matched healthy control groups (Figure 1a–c). In PD patients, the DAT bindings in caudate were greater in the YOPD group (Figure 1a), while the DAT bindings in putamen of YOPD were quite similar to the LOPD groups (Figure

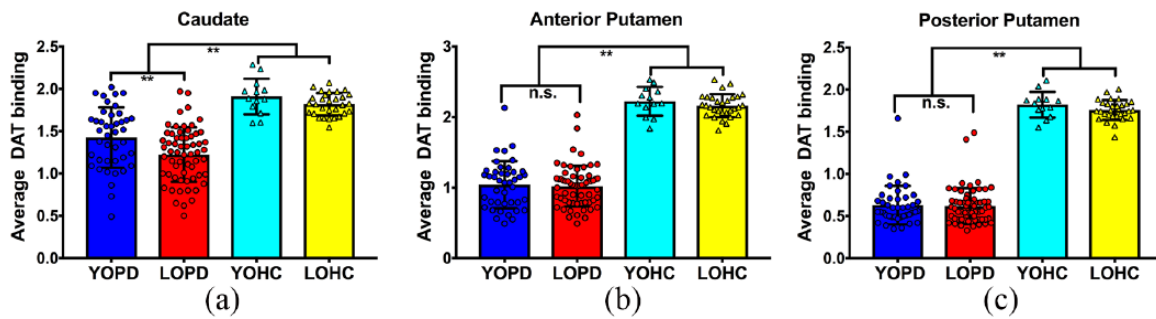


Figure 1. (a) Average dopamine transporter (DAT) binding of caudate in young-onset PD (YOPD) is higher than late-onset PD (LOPD) ($p < 0.01$), and significantly lower than the age-matched healthy controls ($p < 0.01$). (b) and (c) DAT bindings of anterior putamen (b) and posterior putamen (c) in YOPD were as low as LOPD, but significantly lower than the age-matched healthy controls ($p < 0.01$). HC: healthy controls; YOHC: healthy controls to YOPD; LOHC: healthy controls to LOPD. ** $p < 0.01$. n.s., nonsignificant.

1b and c). These results suggested that the DAT bindings in caudate were relatively spared in the YOPD group, compared with similar lesions in putamen to LOPD (Figure 1).

The metabolic characteristics in YOPD

Compared with healthy controls of similar age, YOPD patients showed increased metabolism in bilateral basal ganglia, cerebellum, thalamus, and frontal lobes (Figure 2a and Table 2) and decreased metabolism in cuneus, occipital and temporal lobes bilaterally (Figure 2a and Table 2). Compared with healthy controls of older age, the LOPD patients showed metabolism differences (Figure 2b) similar to those we found in YOPD patients. The regions with metabolism changes were similar to the regions reported in Parkinson's disease related pattern (PDRP).²³

In comparison with LOPD patients, YOPD patients showed hypermetabolism in the caudate, medial frontal gyrus (BA 25), and anterior cingulate (Figure 2c and Table 3). Moreover, the YOPD group exhibited decreased metabolism in bilateral putamen (Figure 2c and Table 3). In the *post hoc* analysis, the rCMR_{glc} values were extracted from caudate (12, 8, 8) and putamen (28, -20, 14). The metabolic values of caudate in YOPD group were significantly higher than the LOPD group (Figure 2d), and metabolic values of putamen were significantly lower than the LOPD group (Figure 2e). Furthermore, the metabolic values in caudate were similar to age-matched healthy controls, but the metabolic

values in putamen were higher than age-matched healthy controls.

Correlation analysis of ¹⁸F-FDG and ¹¹C-CFT PET imaging

In ¹¹C-CFT PET imaging, DAT bindings of caudate were higher in YOPD than LOPD, although the DAT bindings of putamen were similar between the two groups. In ¹⁸F-FDG PET imaging, YOPD patients showed increased metabolism in the caudate and decreased metabolism in putamen than LOPD. In the following correlation study, the normalized metabolic value in caudate detected in ¹⁸F-FDG PET imaging correlated with the DAT binding in caudate (Figure 2f). The correlations found between ¹⁸F-FDG and ¹¹C-CFT PET imaging supported our findings that the caudate function was relatively preserved in YOPD patients. Furthermore, the dopaminergic and metabolic values in caudate correlated moderately with the scores of CWT-C and TMT-A tests (Supplementary Figure S1).

Discussion

In this dual-tracer PET study, we identified the preserved caudate function and better cognition in YOPD. In ¹¹C-CFT PET scans, the YOPD cohort exhibited a less impaired dopaminergic function in caudate than putamen, compared with the DAT bindings of caudate and putamen in LOPD. In ¹⁸F-FDG PET scans, patients of YOPD showed increased metabolism in basal

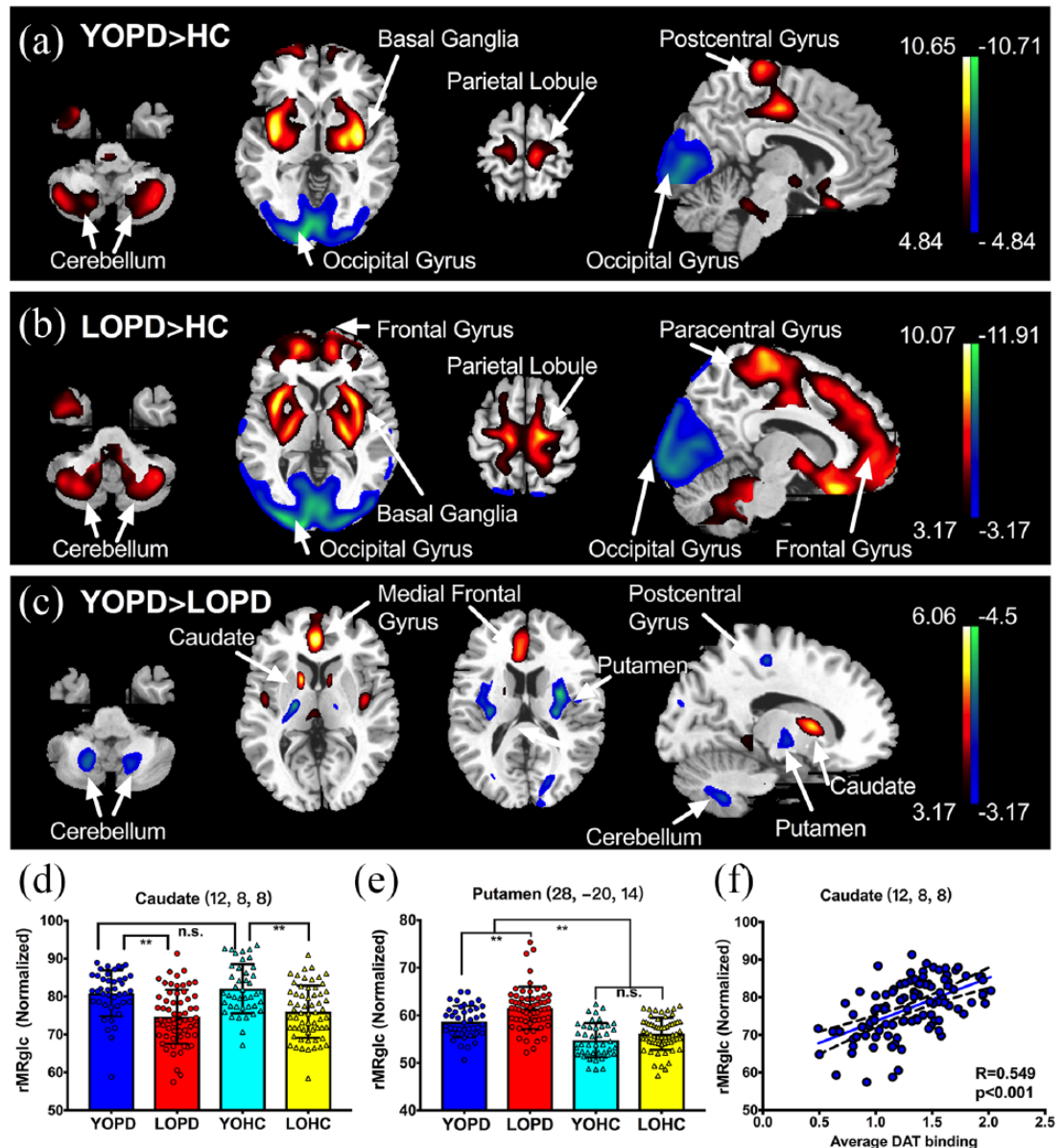


Figure 2. Brain regions exhibiting metabolic differences between (a) YOPD and HC, (b) LOPD and HC, and (c) YOPD and LOPD. Regions of increased metabolism are displayed as a red–yellow scale, decreased metabolism as a blue–purple scale. The colored stripe indicates the *t*-value; voxel threshold $p < 0.001$. Coordinates are displayed in Montreal Neurological Institute (MNI) standard space. (d) Normalized regional cerebral metabolic rate of glucose (rCMRglc) values of caudate in young onset Parkinson’s disease (YOPD) (blue) were significantly higher than in late onset Parkinson’s disease (LOPD) (red) ($p < 0.01$), both being similar to age-matched healthy controls [healthy controls to YOPD (YOHC), green; healthy controls to LOPD (LOHC), yellow]. (e) rCMRglc values of putamen in YOPD (blue) were significantly lower than LOPD (red) ($p < 0.01$), both being significantly higher than in age-matched healthy controls ($p < 0.01$) (YOHC, green; LOHC, yellow). (f) Normalized rCMRglc values of caudate correlated well with the average dopaminergic binding in caudate. $**p < 0.01$. n.s., nonsignificant.

ganglia than healthy controls. Compared with the LOPD, YOPD patients showed increased metabolism in caudate but decreased metabolism in putamen. Furthermore, the normalized caudate metabolic values correlated significantly with

DAT binding values of caudate, which further corroborated our findings. Taken together, our study suggested a relative sparing of caudate compared with putamen in YOPD, which correlated with better cognitive function.

Table 2. Brain regions with significant metabolic difference between the YOPD patients and age-matched healthy controls.

Metabolism	Regions	BA	Cluster Size (mm ³)*	Z max	MNI Coordinates ^a		
					X	Y	Z
Increased*	Left Inferior Frontal Gyrus**	47	429,080	9.69	-18	18	-22
	Right Inferior Parietal Lobule	40	2568	4.11	64	-26	32
	Right Postcentral Gyrus	1	2568	3.78	68	-16	26
	Left Claustrum extended to Putamen and Caudate**	/	429,080	10.71	-36	-10	2
	Right Claustrum extended to Putamen and Caudate**	/	429,080	10.47	38	-6	2
Decreased*	Right Cuneus**	17	143,712	7.47	14	-100	0
	Right Middle Occipital Gyrus**	18	143,712	7.46	28	-92	2
	Left Superior Temporal Gyrus	41	5264	4.07	-58	-26	8
	Right Superior Temporal Gyrus	22	1592	4.46	56	-42	8

BA: Brodmann Area; YOPD: Young-onset Parkinson's disease; MNI: Montreal Neurological Institute; FWE Family-Wise-Error.
^aCoordinates are displayed in MNI standard space.
*Significant at voxel threshold of $p < 0.001$, extent threshold = 95 voxels (760 mm³), **survived after FWE correction, $p < 0.05$.

Table 3. Brain regions with significant metabolic difference between the YOPD and LOPD patients.

Metabolism	Regions	BA	Cluster size (mm ³)*	Z max	MNI coordinates ^a		
					X	Y	Z
Increased*	Right Medial Frontal Gyrus	25	31,536	5.07	4	24	-16
	Right Anterior Cingulate	32	31,536	5.77	2	42	0
	Right Caudate	/	32,563	5.76	12	8	8
Decreased*	Left Insula extended to putamen	13	7088	4.73	-32	-12	20
	Right Putamen	/	8656	4.55	28	-20	14

BA: Brodmann Area; LOPD: Late-onset Parkinson's disease; YOPD: Young-onset Parkinson's disease; MNI: Montreal Neurological Institute; FWE Family-Wise-Error.
^aCoordinates are displayed in MNI standard space.
*Significant after FWE correction, $p < 0.05$, extent threshold = 90 voxels (720 mm³).

Dysfunctional cortico-striato-thalamo-cortical circuitry in YOPD patients

In ¹⁸F-FDG PET, YOPD patients showed hypermetabolism in basal ganglia, which was quite similar to the previously reported metabolic changes in PDRP.²³ Compared with LOPD, YOPD

patients displayed increased metabolism in caudate, medial frontal gyrus, and anterior cingulate (Table 3). Prior research had illustrated that the dysfunction of frontal-striatal circuit, which included dopaminergic impairment in caudate and metabolic changes in prefrontal lobe and

anterior cingulate, contributed to the poor cognitive performances of PD patients.²⁷ Functional connectivity studies also supported that collaborative activation of caudate and neocortex is essential for normal cognitive status.²⁸ In this study, the brain regions detected could potentially be classified as cognition-related brain regions. In our patients with cognition tests, the YOPD group performed better than LOPD patients of similar disease duration in attention and executive functions. After adjusting for age effects, better attention and executive functions could also be found in YOPD (Table 3 and Supplementary Table S3). Furthermore, the metabolism values in caudate correlated moderately with the scores of CWT-C and TMT-A tests (Figure 3). In this regard, unharmed synchrony of frontal-striatal neuronal activity probably explained the lesser cognitive dysfunction in YOPD patients.

In the present study, YOPD patients displayed decreased metabolism than LOPD patients in putamen. It was reported that YOPD patients exhibited more profound damage in striatum at the first appearance of symptoms, due to more effective compensatory mechanisms.^{29,30} This might partially explain the hypometabolism in putamen observed in our study.

YOPD exhibited a different dopaminergic disruptive pattern in striatum than LOPD

In the present study, the DAT binding values of putamen in the YOPD group were as low as in the LOPD group, but the DAT binding values of caudate in YOPD were much higher. The less impaired caudate than putamen in YOPD could be supported by the fact that putamen and caudate received different dopaminergic projections from *substantia nigra*. In a microarchitecture study of *substantia nigra*, the dorsal putamen received projections mainly from the lateral ventral tier of *substantia nigra*, which is selectively and most prominently impaired in PD.^{31,32} In contrast, caudate accepted projections mainly from medial lateral part of *substantia nigra*, which was reported to be less severely affected in nondemented PD patients.³³ The relative sparing of caudate in dopaminergic imaging was in accordance with the finding that YOPD patients were less likely to have cognitive decline,³ and this could be further

supported by our cognitive data in YOPD and LOPD patients.

The greater sparing of caudate than putamen in YOPD patients might also be explained by the uneven degree of involvement of caudate and putamen in the parallel basal ganglio-thalamo-cortical circuits. Putamen-related motor circuits were responsible for motor functions, and disruption of putamen function correlated well with the onset of cardinal motor symptoms³⁴ and motor severities,^{10,35} whereas caudate was more likely to be involved in the circuits related to cognitive and affective functions.^{36–38} Patients with caudate lesion suffered from cognitive changes, including poor planning and sequencing.³⁹ In the current study, DAT binding in caudate correlated moderately with TMT-A test scores. In a previous cognition study in PD, only the DAT binding in caudate but not putamen correlated significantly with the Parkinson's disease-related cognitive pattern (PDCP).⁴⁰ As previously reported, YOPD patients had a relatively good cognitive status despite more substantial impairment to the motor function.³ The dissociations between putamen and caudate related circuits and clinical manifestations further supported the uneven disruptive patterns in striatum of YOPD.

Dopamine deficiency correlated with metabolic anomalies within the striatum in YOPD

In the correlation analysis between the two imaging studies, we noticed a modest correlation between metabolic values of caudate and DAT binding values of caudate. Therefore, we believe that the uneven lesion in caudate detected in both metabolic and dopaminergic imaging were in accordance with each other. Previously, altered levels of glucose metabolism was reported to correlate with dopaminergic depletion in the caudate and putamen.⁴¹ Some studies suspected nigrostriatal dopamine deficiency as the cause of abnormal synaptic activities within this region,⁴² and local synaptic activity was a reflection of glucose consumption.^{10,43} In this vein, the modest consistency of caudate of both dopaminergic and metabolic measurement exhibited by YOPD patients were interconnected, supporting the characteristic uneven disruptive patterns of striatum in young and late onset-related PD subtypes.

Discrepant degeneration of striatum might provide insights for clinical practice

Although there is no well-accepted robust criterion for subtyping PD, the uneven disruptive patterns in striatum of YOPD detected in both dopaminergic and metabolic imaging highly support the necessity to consider the age of onset in further clinical trials of novel treatments. We supposed that the uneven injury of caudate and putamen between YOPD and LOPD might be related to the uneven lesion in cognition and motor functions. Thus, these findings may offer valuable information towards developing more precise strategies in different onset-related subtypes of PD. First, YOPD and LOPD might respond differently to treatment for different symptoms. Second, functional neuroimaging parameters may not be suitable as primary biomarkers without controlling for the effects of onset age. In contrast, recruiting patients of homogeneous age of onset might reduce variability, and may also decrease sample sizes with increased statistical power.

Strengths and limitations

In this dual-tracer PET imaging cohort of PD patients, we aimed to detect dopaminergic and metabolic characteristics of YOPD. In this cohort, an analogous metabolic distribution similar to that found in dopaminergic system dysfunction was reported, which was further supported by the correlation analysis. The dual-tracer PET imaging in the same cohort made the disruptive pattern in striatum more acceptable.

Our study detected a series of brain regions reported to be involved in cognition function. These findings make sense as cognition in YOPD is relatively conserved. However, only a subset of participants in our study performed the comprehensive cognition tests, which might restrict a deeper understanding of our imaging findings. Some FWE-uncorrected clusters that survived only at $p < 0.001$ but have been previously reported were also presented in our study, which could be accepted in hypothesis-testing analysis but are a bit weak. Although we conducted this dual-tracer imaging study, we may have underestimated the nondopaminergic pathway, which could contribute to some nonmotor differences between the two subtypes.⁴⁴ Another limitation of this study was that results of genetic abnormality were not included. We admit that genetic factors contribute to the cause of YOPD, but the absence

of genetic data does not undermine the existing dopaminergic and metabolic patterns. We are conducting ongoing research regarding the genetic influence on the onset-related subtypes of Parkinson's disease that will not be discussed here.

Conclusion

This novel dual-tracer study indicated the uneven injuries of caudate and putamen between YOPD and LOPD in the striatum, basing on the dopaminergic and glucose metabolic PET imaging differences. These characteristics might be related to the uneven lesion in cognition and motor functions between YOPD and LOPD. In conclusion, our findings may offer some valuable information towards more precise strategies in different onset-related subtypes of PD in general clinical practice.

Acknowledgements

Authors Yu-jie Yang, Jing-jie Ge and Feng-tao Liu contributed equally.

Author contribution

The authors' roles in the project and preparation of the article are as follows. Research project: conception by JW, CTZ, YLM, and FTL; organization by YJY, JJG, ZYL, and JJW; execution by YJY, JJG, ZYL and JZ. Statistical analysis: design by JW and CTZ; execution by YJY, FTL, and JJG; review and critique by JW, CTZ, and YLM. Manuscript: writing of the first draft by YYJ, FTL, JJG, and JJW; review and critique by JW, CTZ, and JJW.

Funding

This work was supported by Ministry of Science and Technology of China [grant number: 2016YFC1306500, 2016YFC1306504], the National Nature Science Foundation of China [grant number: 81701250, 81771372, 81671239, 81571232, 81361120393], Shanghai Municipal Commission of Science and Technology (grant number: 2018SHZDZX01, 17JC1401400), the Open Project Funding of Human Phenome Institute, Fudan University (grant number: HUPIKF2018203), China Postdoctoral Science Foundation [grant number: 2017M610227, 2018T110350], and Shanghai Sailing Program [No. 18YF1403100].

Conflict of interest statement

The authors declare that there is no conflict of interest.

Supplemental material

Supplemental material for this article is available online.

ORCID iD

Jian Wang  <https://orcid.org/0000-0001-9952-0898>

References

- Berg D, Postuma RB, Bloem B, *et al.* Time to redefine PD? Introductory statement of the MDS Task Force on the definition of Parkinson's disease. *Mov Disord* 2014; 29: 454–462.
- Pagano G, Ferrara N, Brooks DJ, *et al.* Age at onset and Parkinson disease phenotype. *Neurology* 2016; 86: 1400–1407.
- Wickremaratchi M, Ben-Shlomo Y and Morris HR. The effect of onset age on the clinical features of Parkinson's disease. *Eur J Neurol* 2009; 16: 450–456.
- Knipe MDW, Wickremaratchi MM, Wyatt-Haines E, *et al.* Quality of life in young-compared with late-onset Parkinson's disease. *Mov Disord* 2011; 26.
- Schrag A and Schott JM. Epidemiological, clinical, and genetic characteristics of early-onset parkinsonism. *Lancet Neurol* 2006; 5: 355–363.
- Mehanna R, Moore S, Hou JG, *et al.* Comparing clinical features of young onset, middle onset and late onset Parkinson's disease. *Parkinsonism Relat Disord* 2014; 20: 530–534.
- Kempster PA, O'Sullivan SS, Holton JL, *et al.* Relationships between age and late progression of Parkinson's disease: a clinico-pathological study. *Brain* 2010; 133: 1755–1762.
- Tang H, Huang J, Nie K, *et al.* Cognitive profile of Parkinson's disease patients: a comparative study between early-onset and late-onset Parkinson's disease. *Int J Neurosci* 2016; 126: 227–234.
- Attwell D and Iadecola C. The neural basis of functional brain imaging signals. *Trends Neurosci* 2002; 25: 621–625.
- Liu FT, Ge JJ, Wu JJ, *et al.* Clinical, dopaminergic, and metabolic correlations in Parkinson disease: a dual-tracer PET study. *Clin Nucl Med* 2018; 43: 562–571.
- Gibb WR and Lees AJ. The relevance of the Lewy body to the pathogenesis of idiopathic Parkinson's disease. *J Neurol Neurosurg Psychiatry* 1988; 51: 745–752.
- Quinn N, Critchley P and Marsden CD. Young onset Parkinson's disease. *Mov Disord* 1987; 2: 73–91.
- Tanner CM, Ottman R, Goldman SM, *et al.* Parkinson disease in twins: an etiologic study. *JAMA* 1999; 281: 341–346.
- Liu SY, Wu JJ, Zhao J, *et al.* Onset-related subtypes of Parkinson's disease differ in the patterns of striatal dopaminergic dysfunction: a positron emission tomography study. *Parkinsonism Relat Disord* 2015; 21: 1448–1453.
- Fahn S, Oakes D, Shoulson I, *et al.* Levodopa and the progression of Parkinson's disease. *N Engl J Med* 2004; 351: 2498–2508.
- Litvan I, Goldman JG, Troster AI, *et al.* Diagnostic criteria for mild cognitive impairment in Parkinson's disease: Movement Disorder Society Task Force guidelines. *Mov Disord* 2012; 27: 349–356.
- Zhao Q, Guo Q, Li F, *et al.* The Shape Trail Test: application of a new variant of the Trail making test. *PLoS One* 2013; 8: e57333.
- Sheridan LK, Fitzgerald HE, Adams KM, *et al.* Normative Symbol Digit Modalities Test performance in a community-based sample. *Arch Clin Neuropsychol* 2006; 21: 23–28.
- Steinberg BA, Bieliauskas LA, Smith GE, *et al.* Mayo's Older Americans Normative Studies: Age- and IQ-Adjusted norms for the Trail-Making Test, the Stroop Test, and MAE Controlled Oral Word Association Test. *Clin Neuropsychol* 2005; 19: 329–377.
- Guo Q, Zhao Q, Chen M, *et al.* A comparison study of mild cognitive impairment with 3 memory tests among Chinese individuals. *Alzheimer Dis Assoc Disord* 2009; 23: 253–259.
- Caffarra P, Vezzadini G, Dieci F, *et al.* Rey-Osterrieth complex figure: normative values in an Italian population sample. *Neurol Sci* 2002; 22: 443–447.
- Lucas JA, Ivnik RJ, Smith GE, *et al.* Mayo's Older African Americans normative studies: norms for Boston Naming Test, Controlled Oral Word Association, Category Fluency, Animal Naming, Token Test, WRAT-3 Reading, Trail Making Test, Stroop Test, and Judgment of Line Orientation. *Clin Neuropsychol* 2005; 19: 243–269.
- Wu P, Wang J, Peng S, *et al.* Metabolic brain network in the Chinese patients with Parkinson's disease based on 18F-FDG PET imaging. *Parkinsonism Relat Disord* 2013; 19: 622–627.

24. Zuo C, Ma Y, Sun B, *et al.* Metabolic imaging of bilateral anterior capsulotomy in refractory obsessive compulsive disorder: an FDG PET study. *J Cereb Blood Flow Metab* 2013; 33: 880–887.
25. Bu LL, Liu FT, Jiang CF, *et al.* Patterns of dopamine transporter imaging in subtypes of multiple system atrophy. *Acta Neurol Scand* 2018; 138: 170–176.
26. Huang C, Tang C, Feigin A, *et al.* Changes in network activity with the progression of Parkinson's disease. *Brain* 2007; 130: 1834–1846.
27. Gratwicke J, Jahanshahi M and Foltynic T. Parkinson's disease dementia: a neural networks perspective. *Brain* 2015; 138: 1454–1476.
28. Postuma RB and Dagher A. Basal ganglia functional connectivity based on a meta-analysis of 126 positron emission tomography and functional magnetic resonance imaging publications. *Cereb Cortex* 2006; 16: 1508–1521.
29. de la Fuente-Fernández R, Schulzer M, Kuramoto L, *et al.* Age-specific progression of nigrostriatal dysfunction in Parkinson's disease. *Ann Neurol* 2011; 69: 803–810.
30. Shih MC, de Andrade F, Augusto L, *et al.* Higher nigrostriatal dopamine neuron loss in early than late onset Parkinson's disease?—A [99mTc]-TRODAT-1 SPECT study. *Mov Disord* 2007; 22: 863–866.
31. Wu T, Wang L, Hallett M, *et al.* Effective connectivity of brain networks during self-initiated movement in Parkinson's disease. *NeuroImage* 2011; 55: 204–215.
32. Fearnley JM and Lees AJ. Ageing and Parkinson's disease: substantia nigra regional selectivity. *Brain* 1991; 114: 2283–2301.
33. Rinne JO, Rummukainen J, Paljarvi L, *et al.* Dementia in Parkinson's disease is related to neuronal loss in the medial substantia nigra. *Ann Neurol* 1989; 26: 47–50.
34. Rodriguez-Oroz MC, Jahanshahi M, Krack P, *et al.* Initial clinical manifestations of Parkinson's disease: features and pathophysiological mechanisms. *Lancet Neurol* 2009; 8: 1128–1139.
35. Broussolle E, Dentresangle C, Landais P, *et al.* The relation of putamen and caudate nucleus 18 F-dopa uptake to motor and cognitive performances in Parkinson's disease. *J Neurol Sci* 1999; 166: 141–151.
36. DeLong MR and Wichmann T. Basal ganglia circuits as targets for neuromodulation in Parkinson disease. *JAMA Neurol* 2015; 72: 1354–1360.
37. DeLong M and Wichmann T. Update on models of basal ganglia function and dysfunction. *Parkinsonism Relat Disord* 2009; 15(Suppl. 3): S237–S240.
38. Wu L, Liu FT, Ge JJ, *et al.* Clinical characteristics of cognitive impairment in patients with Parkinson's disease and its related pattern in (18) F-FDG PET imaging. *Hum Brain Mapp* 2018; 39: 4652–4662.
39. Mendez MF, Adams NL and Lewandowski KS. Neurobehavioral changes associated with caudate lesions. *Neurology* 1989; 39: 349–354.
40. Niethammer M, Tang CC, Ma Y, *et al.* Parkinson's disease cognitive network correlates with caudate dopamine. *Neuroimage* 2013; 78: 204–209.
41. Holtbernd F, Ma Y, Peng S, *et al.* Dopaminergic correlates of metabolic network activity in Parkinson's disease. *Hum Brain Mapp* 2015; 36: 3575–3585.
42. Eggers C, Schwartz F, Pedrosa DJ, *et al.* Parkinson's disease subtypes show a specific link between dopaminergic and glucose metabolism in the striatum. *PLoS One* 2014; 9: e96629.
43. Eidelberg D, Moeller JR, Kazumata K, *et al.* Metabolic correlates of pallidal neuronal activity in Parkinson's disease. *Brain* 1997; 120: 1315–1324.
44. Chaudhuri KR, Healy DG and Schapira AH National Institute for Clinical Excellence. Non-motor symptoms of Parkinson's disease: diagnosis and management. *Lancet Neurol* 2006; 5: 235–245.